Seismic Attenuation for Reservoir Characterization

DE-FC26-01BC15356

Quarterly Report
Apr. 1 – June 30, 2002

Issued July, 2002

Contributors

Dr. Joel Walls*

Dr. M. T. Taner*

Dr. Gary Mavko**

Dr. Jack Dvorkin**

*Principal Contractor:

Rock Solid Images

2600 S. Gessner Suite 650

Houston, TX, 77036

**Subcontractor:

Petrophysical Consulting Inc.

730 Glenmere Way

Emerald Hills, CA, 94062

Disclaimer

Contents

SECTION 1: ATTENUATION AT FULL WATER SATURATION

ABSTRACT

In fully-saturated rock and at ultrasonic frequencies, the microscopic squirt flow induced between the stiff and soft parts of the pore space by an elastic wave is responsible for velocity–frequency dispersion and attenuation. In the seismic frequency range, it is the macroscopic cross-flow between the stiffer and softer parts of the rock. We use the latter hypothesis to introduce simple approximate equations for velocity-frequency dispersion and attenuation in a fully water saturated reservoir. The equations are based on the assumption that in heterogeneous rock and at a very low frequency, the effective elastic modulus of the fully-saturated rock can be estimated by applying a fluid substitution procedure to the averaged (upscaled) dry frame whose effective porosity is the mean porosity and the effective elastic modulus is the Backus-average (geometric mean) of the individual *dry-frame* elastic moduli of parts of the rock. At a higher frequency, the effective elastic modulus of the saturated rock is the Backus-average of the individual *fully-saturated-rock* elastic moduli of parts of the rock. The difference between the effective elastic modulus calculated separately by these two methods determines the velocity-frequency dispersion. The corresponding attenuation is calculated from this dispersion by using (e.g.) the standard linear solid attenuation model.

UPPER AND LOWER ELASTIC LIMITS AT FULL SATURATION

Let us assume that a heterogeneous domain of rock includes a number of homogeneous parts with porosity f and the dry-frame compressional modulus M_{Dry} that vary among those parts but are constant within each individual part. Then the effective porosity f_{Eff} of the domain is the arithmetic average of individual porosities:

$$f_{Eff} = \langle f \rangle, \tag{1}$$

and the effective dry-frame compressional modulus is the Backus (geometric) average of individual moduli:

$$M_{DryEff} = \left\langle M_{Dry}^{-1} \right\rangle^{-1}. \qquad (2)$$

At a very low frequency and in saturated rock, the wave-induced pressure increments equilibrate between the individual parts. As a result, the effective saturated-rock compressional modulus can be calculated by applying the *P*-only fluid substitution equation (Mavko et al., 1995) to the entire domain under examination:

$$M_{SatEff0} = M_S \frac{\phi_{Eff} M_{DryEff} - (1+\phi_{Eff}) K_F M_{DryEff} / M_S + K_F}{(1-\phi_{Eff}) K_F + \phi_{Eff} M_S - K_F M_{DryEff} / M_S}, \qquad (3)$$

where M_S is the mineral-phase compressional modulus, assumed the same for all individual parts of the rock; and K_F is the bulk modulus of the pore fluid, also the same throughout the heterogeneous domain.

At a higher frequency, the individual parts of the domain are undrained. The saturated-rock compressional moduli of each individual part can be calculated by applying the *P*-only fluid substitution equation individually. Then the effective saturated-rock compressional modulus is the Backus average of the individual saturated-rock compressional moduli:

$$M_{SatEff\infty} = \left\langle (M_S \frac{\phi M_{Dry} - (1+\phi) K_F M_{Dry} / M_S + K_F}{(1-\phi) K_F + \phi M_S - K_F M_{Dry} / M_S})^{-1} \right\rangle^{-1}. \qquad (4)$$

Consider an example where the heterogeneous domain includes two clean-sand individual parts of equal volumes. The porosities of the two parts are 0.35 and 0.30, the respective dry-frame *P*-wave velocities are and 2.3 km/s and 2.9 km/s, and the respective dry-frame compressional moduli are 9.11 GPa and 15.6 GPa. The compressional modulus of the solid phase (quartz) is 100 GPa and the bulk modulus of the pore fluid (brine) is 2.7 GPa.

The effective porosity, according to Equation (1), is 0.325 and the effective dry-frame compressional modulus, according to Equation (2), is 11.5 GPa. The corresponding low-frequency saturated-rock compressional modulus $M_{SatEff0}$ is, according to Equation (3), 17.7 GPa.

The individual saturated-rock compressional moduli of the parts of the rock are 15.2 GPa and 21.7 GPa for porosity 0.35 and 0.3, respectively. Then the corresponding high-frequency saturated-rock compressional modulus $M_{SatEff\infty}$ is, according to Equation (4), 17.9 GPa.

The corresponding maximum inverse quality factor, according to the standard linear solid model,

$$(\frac{1}{Q})_{\max} = \frac{M_\infty - M_0}{2\sqrt{M_0 M_\infty}}, \tag{5}$$

is 0.0056.

INVERSE QUALITY FACTOR FROM WELL LOG DATA

Exactly the same approach can be used if well log data are available. First, the dry-frame compressional modulus is calculated from the original log data as

$$M_{Dry} = M_S \frac{1-(1-f)M_{Sat}/M_S - fM_{Sat}/K_F}{1+f-fM_S/K_F - M_{Sat}/M_S}, \tag{6}$$

where M_{Sat} is the product of the measured bulk density and the *P*-wave velocity squared.

Then the above-described operation is applied to calculate $M_{SatEff0}$, $M_{SatEff\infty}$, and the maximum inverse quality factor. The averaging required can be done along a moving window of a desired length, corresponding, e.g., to a quarter-wavelength.

An example of such calculation is given in Figure 1 for a 1-km-long shaley interval. The resulting inverse quality factor appears to lie within a reasonable range between 0.01 and 0.02 which corresponds to the quality factor between 50 and 100.

EFFECT OF SAMPLING IN WELL LOG DATA

An important issue is the stability of the proposed attenuation calculation method with respect to the sampling interval in well log curves. Will the calculated attenuation be the same if the sampling rate is a half foot, a 1 foot, and two feet?

To address this issue we subsampled the original well log data used in Figure 1,

whose sampling is a half-foot, with (a) a one-foot interval, and (b) a two-foot interval.

The resulting inverse quality factor is plotted versus depth in the fifth frame of Figure 1. It is essentially identical to that computed from the data with the original (half-foot) sampling rate.

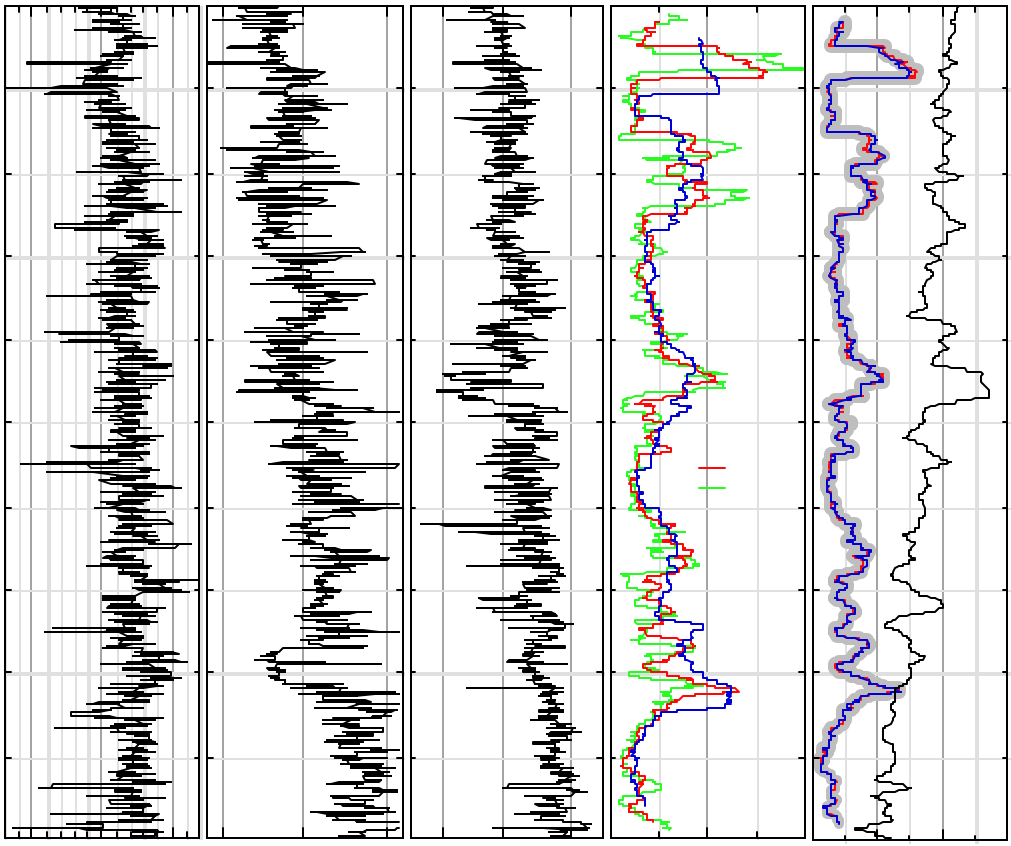

Figure 1. First three frames -- well log data from a water-saturated interval (gamma ray, *P*-wave velocity, and bulk density). Fourth frame -- calculated inverse *P*-wave quality factor for three sizes of running window – 75, 38, and 19 m. Fifth frame -- inverse *P*-wave quality factor calculated from undersampled well log data (red and blue) superimposed on the curve calculated from the original data with the 38 m running window (bold gray curve). Also, in the same frame the black curve is the inverse *P*-wave quality factor from the Koesoemadinata and McMechan (2001) empirical model, labeled KOM.

COMPARISON TO AN EMPIRICAL MODEL

The Koesoemadinata and McMechan (2001) model (KOM) is simply a statistical regression to most of the available attenuation data. Unfortunately, no data are available

in the seismic frequency range which makes this regression no more than a guess at seismic frequency. Nevertheless, we compare our modeling results to those predicted by KOM, the latter applied to the well log data shown in Figure 1 and assuming constant (50%) clay content and 30 Hz frequency. The KOM inverse quality factor (Figure 1, fifth frame) is larger than that predicted by our model. Still, both curves lie in the same range which indirectly indicates the relevance of the rational model introduced here.

CONCLUSION

Attenuation remains an elusive propagational seismic attribute that is hard to measure and theoretically model. This paper presents an attempt to model attenuation in fully saturated rock using a simple theoretical approach and first physical principles. The main purpose of modeling is not just to predict attenuation but to establish what can be said about the reservoir properties from attenuation. In other words, our aspiration is to make attenuation a reservoir characterization tool. In our previous report (second quarter 2002) we proposed that attenuation is a measure of gas saturation. Present work implies that in fully-saturated rock, *attenuation is a measure of elastic heterogeneity.*

The model introduced here has to be validated by real data which only can come from attenuation calculated from seismic.

SECTION 2: RELATIVE Q COMPUTATION BY SPECTRAL BALANCING

INTRODUCTION:

We have included the spectral balancing by the Gabor-Morlet decomposition as a part of the software developed for compensating the Q effects. The results are very well formed and the process is stable. This shows that the procedure is adaptively adjusting the seismic trace spectra as the process advances in time. While discussing the process with Dr. Walls, it appeared that the corrections applied to the seismic trace can be used to estimate the apparent Q. Such a process was suggested by Dr. Koehler in early 1980's, but we did not attempt to develop it further. Now, due to computational difficulties, we are interested in developing the absorption estimation as many different ways as possible. Since we have a stable spectral balancing procedure, we assume that the related apparent Q computation should also be reasonably stable. We have both agreed to develop the method further and check its accuracy with controlled experiments.

METHOD:

A) SPECTRAL BALANCING:

Given seismic trace, we compute Joint Time-Frequency decomposition by the Gabor-Morlet method.(Taner,2001). The process provides amplitude spectra (as the envelope of complex sub-band traces) for each sub-band continuously in time. A scalar is computed from the ratio between the original trace envelope and sub-band envelopes. The ratio is computed over a running long window and applied to the sub-band traces. Amplitude modified sub-band traces are summed to form the spectrally balanced output traces. By balancing with respect to the original trace amplitude profile, all amplitude relations are preserved, only the wavelet bandwidth is extended and balanced. Spectral balanced sections are used as input to band limited relative acoustic impedance inversions. Our experiments with a number of sections from different parts of the world have shown that spectral balancing and band limited inversion works well and is stable.

B) Q ESTIMATION:

We will investigate several processes before finalizing the development of the method. The objective is to compute relative Q from the spectral balancing scalars. Since absorption reduces the amplitudes of higher frequencies more than lower frequencies, the correction scalars will have inverse characteristics of the absorption effects. We will observe the following;

1) Given seismic trace, generate and display joint tome-frequency amplitude spectra, Let f(t), E(t) be the seismic trace and its envelope, and s(f,t), e(f,t) represent the sub-band trace and its envelope respectively. Decomposition is computed to satisfy;

$$F(t) \cong \sum_{f} s(f,t) \tag{1}$$

Spectral balancing scale factor is computed from;

$$r(f,t) = \sum_{t-T/2}^{t+T/2} E(t) / \sum_{t-T/2}^{t+T/2} e(f,t) \tag{2}$$

where T is time window.. The spectral balanced trace generated by the sum of amplitude adjusted traces;

$$\tilde{F}(t) = \sum_{f} r(f,t)s(f,t) \tag{3}$$

2) Compute and display correction scalars, as given in equation 2. In relative Q estimation we will experiment with time windows of different length. Let us assume that computations along the window axis are performed with a moving time window. For the sake of simplicity, we will omit the time window notation form the following expressions. We will study the attenuation process by the conventional model'

$$e(f,t) = e_0(f,t).a(t).\exp(-pft/Q) \tag{4}$$

where e(f,t) is the envelope magnitude at time t (corresponding to the total energy) , $e_0(t)$ the energy level at the initiation and a(t) absolute value of impedance contrast in time. The trace envelope amplitude will also be decaying with time, and it will be proportional to the a(t). However trace envelope decay will be summed result of the decays at various frequency band, However, the ratio of the trace envelope versus the individual sub-band envelope s will retain the effects of the differing decay amount versus frequency. Since Q also varied with time, then to total effect with time can be express as;

$$e(f,t)/E(t) = e_0(f,t).\exp(-pf\int_{t=0}^{t} dt/Q(t))/E(t) \tag{5}$$

We take the natural log of both sides to the constant and frequency varying parts separated'

$$\ln\{ e(f,t) / E(t)\} = (-\pi f \int_{t=0}^{t} dt / Q(t)) + \ln\{ e_0(t) / E(t)\} \qquad (6)$$

The first term of the right hand side of equation 6 is linear function of integral inverse Q with respect to frequency. The second term is weakly time varying. Let the integral inverse Q be represented by P(y);

$$P(t) = \int_{t=0}^{t} dt / Q(t) \qquad (7)$$

Then the equation 6 can be simplified to;

$$\ln\{ e(f,t) / E(t)\} = -\pi f P(t) + C(t)\} \qquad (8)$$

Note that the natural log of the envelope magnitude ratio is inverse of the scalar computed in equation 2. Hence, the relation can be written as;

$$\ln\{ r(f,t)\} = \pi f P(t) - C(t)\} \qquad (9)$$

We can fit a line to log of the balancing scalars, where C(t) will be intercept and P(t) will be the slope of the line . We can line fit with a running window to obtain P(t) continuously in time. Since P(t) is the accumulated inverse Q effect, then we can solve for Q by taking the derivative of the computed P(t) function;

$$Q^{-1}(t) \cong \partial P(t) / \partial t \qquad (10)$$

Equation 10 gives us the instantaneous Q, (similar to instantaneous velocity) mathematically definable, but physically hard to perceive. A more useful measurement is the interval Q measured over a time interval.'

$$Q^{-1}(t) \cong \{P(t + \Delta t) - P(t)\} / \Delta t \qquad (11)$$

In the development stage we will display all of the intermediate computational stages. This will give us a good idea of the validity of the process and consistency of the data flow.

CONCLUSIONS:

We have given a simple method based on the spectral balancing procedure to compute apparent Q values continuously in time. The method given here is applicable to single trace inputs. Our experience has shown us that Q computation is generally very inconsistent, he results have considerable variations. In order to have more consistent results, it is recommended that Q estimates should be obtained aerially, over a number of neighboring traces. The method outlined in this report will be fast and economical, with

little input from the user. Due to its single trace basis, it can be applied to all kinds of data, 2-D or 3-D.

WORK PLANNED FOR NEXT PERIOD

We have obtained a substantial data set from Burlington Resources and Seitel Data that contains both well logs and seismic data from an offshore Gulf of Mexico gas field. We will be using this data to test both our rock physics models of Q from well logs and the seismic methods. In our next report we will show results from this data set and demonstrate the functionality of the combined forward modeling and seismic inversion processes for Q and attenuation.

PROBLEMS ENCOUNTERED THIS PERIOD

No significant problems have been encountered in our work so far. The only exception is that we have not had as many contributed data sets from industry as we had anticipated. One reason may be that the data quality requirements during this testing phase are fairly onerous. Fortunately, we have the Burlington-Seitel data which seems to be very acceptable.

REFERENCES

Backus, G.F., 1962, Long-wave elastic anisotropy produced by horizontal layering, J. Geophys. Res., 67, 4427-4441.

Koesoemadinata, A.P, and McMechan, G.A., 2001, Empirical estimation of viscoelastic seismic parameters from petrophysical properties of sandstone, Geophysics, 66, 1457-1470.

Mavko, G., Chan, C., and Mukerji, T., 1995, Fluid substitution: Estimating changes in Vp without knowing Vs, Geophysics, 60, 1750-1755.

Taner, M. T., 2001, *Joint Time/Frequency Analysis, Q Quality Factor and Dispersion Computation by Gabor-Morlet Wavelets, or the Gabor-Morlet Transform:* RSI Technical Report